

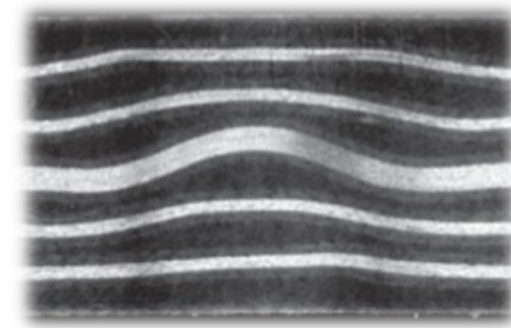
# Evaluation of asymmetric wrinkles using high frequency eddy current and ultrasonic non-destructive testing techniques

Qiuji Yi, Paul Wilcox and Robert Hughes

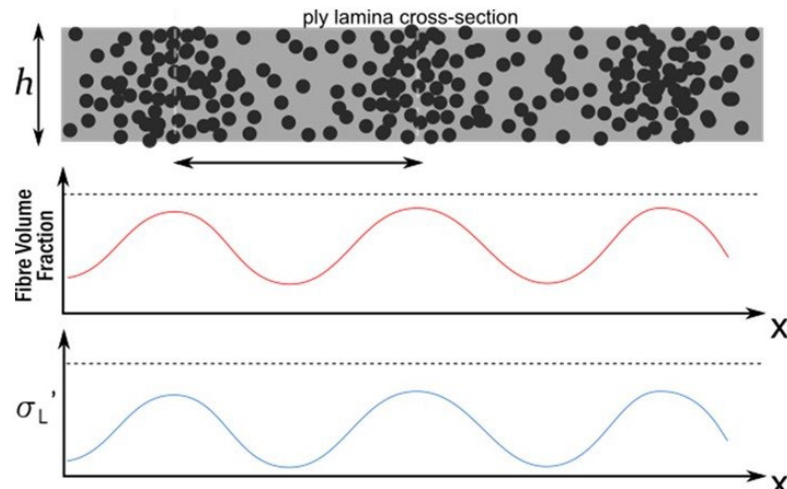
20/01/2022

# Background and motivation

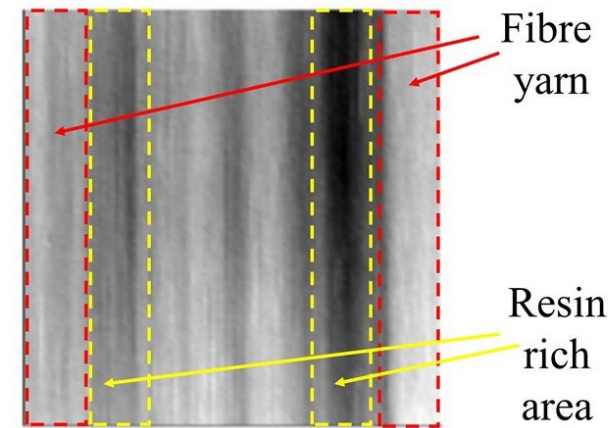
- Eddy currents are excellent for non-contact near-surface detection.
- The first major challenge is the emulation of practical CFRP structure with local heterogeneity caused by the distribution of fibre and resin for optimisation of high-frequency ECT inspections.



Complex wrinkles/Waviness



Simulated conductivity variation in unidirectional CFRP layer



high-resolution ECT image of unidirectional CFRP structure

# Methodology- spatial 'modulation'

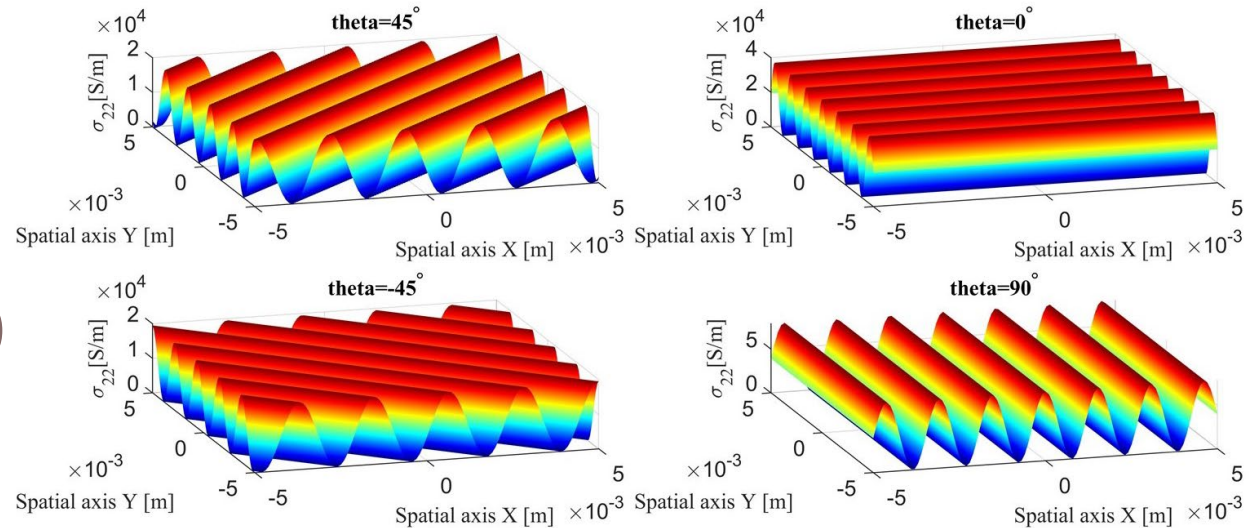
$$\sigma = \begin{Bmatrix} \sigma_{11} & \sigma_{12} & \sigma_{13} \\ \sigma_{21} & \sigma_{22} & \sigma_{23} \\ \sigma_{31} & \sigma_{32} & \sigma_{33} \end{Bmatrix} = \begin{Bmatrix} \sigma_L \cos^2 \theta_f + \sigma_T \sin^2 \theta_f & \frac{\sigma_L - \sigma_T}{2} \sin 2\theta_f & 0 \\ \frac{\sigma_L - \sigma_T}{2} \sin 2\theta_f & \sigma_L \sin^2 \theta_f + \sigma_T \cos^2 \theta_f & 0 \\ 0 & 0 & \sigma_{cp} \end{Bmatrix}$$

The idea is to include a spatial 'modulation' to the conductivity perpendicular to the fibre direction to represent different fibre tows since this modulation enables fibre orientation to be imaged with EC.

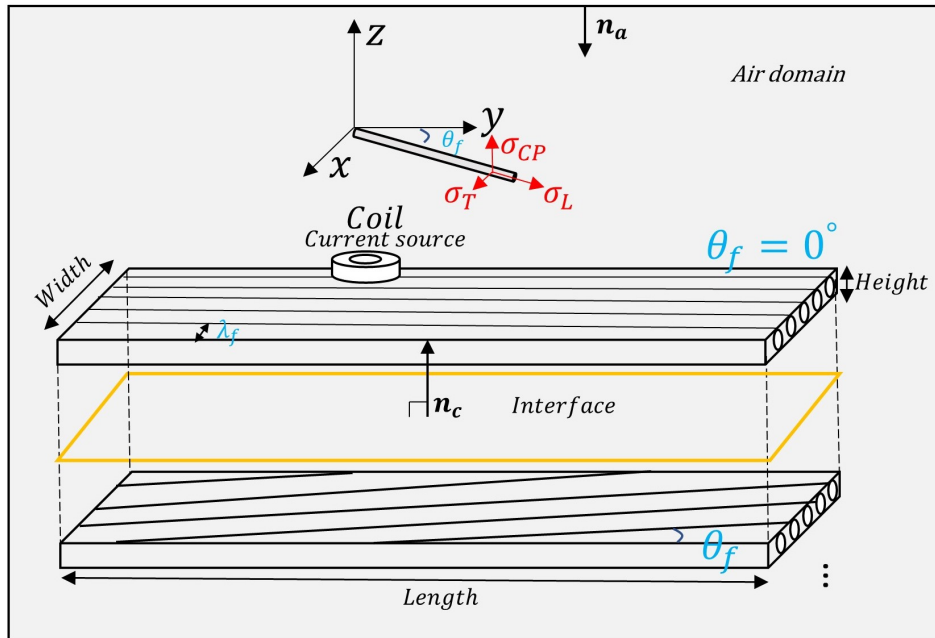
$$\sigma'_{ij}(\theta_f) = \sigma_{ij}(\theta_f) \cdot \frac{A_f(x)}{h} = \sigma_{ij}(\theta_f) \cdot f(x),$$

$$t = x \cos \theta_f - y \sin \theta_f$$

$$\sigma'_{ij}(x, y, \theta_f) = \sigma_{resin} + \frac{\sigma_{ij} - \sigma_{resin}}{2} (1 + \cos \omega_f t)$$



# Methodology- virtual scanning



FEM diagram

The "moving parameter space" method avoids the problem of numerical noise due to the mesh, which was of a similar order to the size of the variations due to simulated fibres.

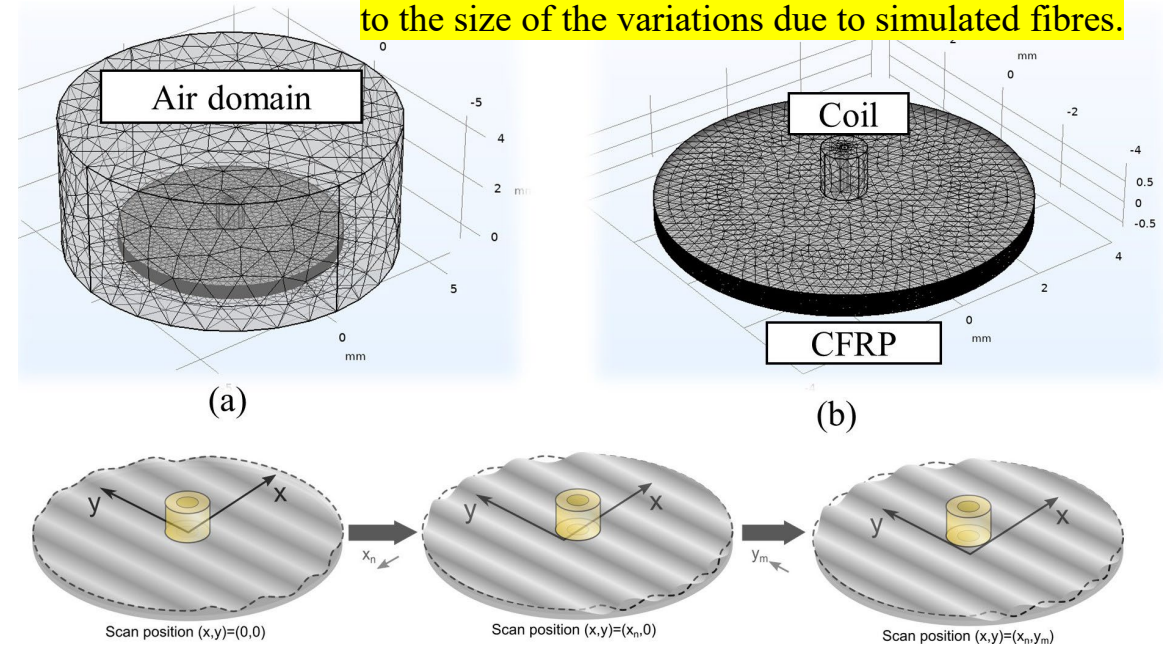
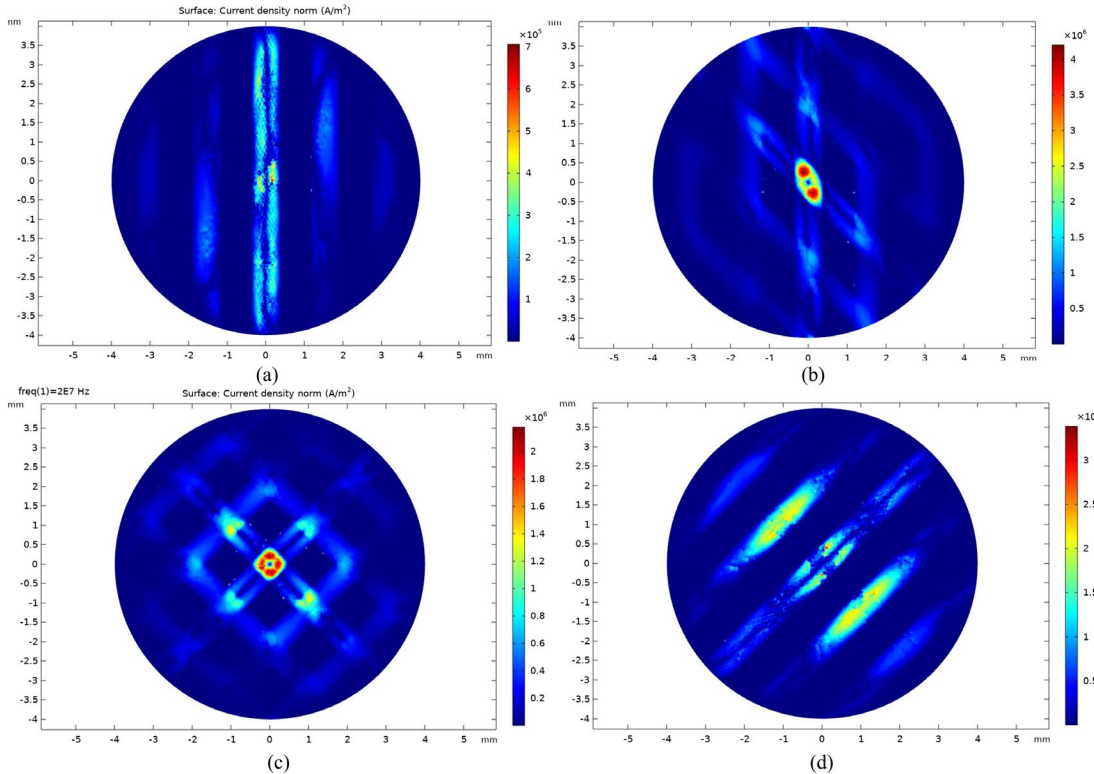


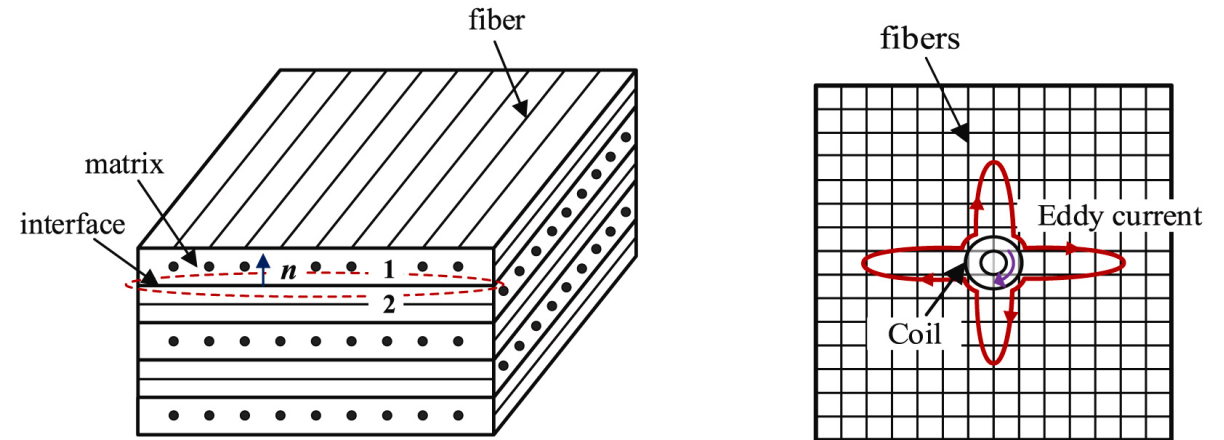
Illustration of moving parameter space

The virtual scanning is implemented by fixing the coil and geometry's position while adding an offset to the parameter space  $\sigma'_{ij}(x, y, \theta_f)$  so that the scanning in X and Y axis can be emulated by  $\sigma'_{ij}(x + x_n, y + y_m, \theta_f)$ , where  $x_n$  and  $y_m$  are the scanning coordinates. This is 5x faster than 'point-by-point' scan.

# Methodology-interface effect



Current density distribution at the surfaces and interfaces in 3-layer sample with [90/-45/45] layup: (a) top surface (90°), (b) interface (90°/-45°), (c) interface (-45°/45°), (d) bottom layer (45°).



Composite laminate

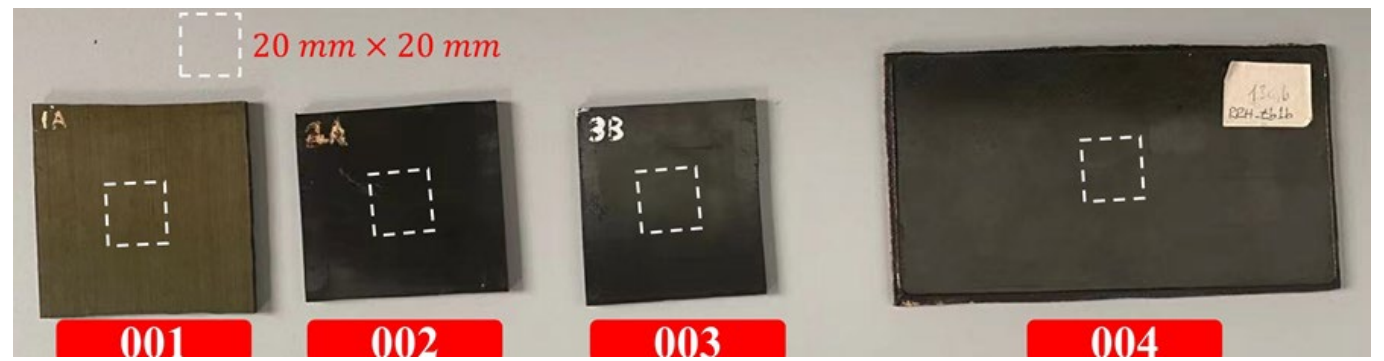
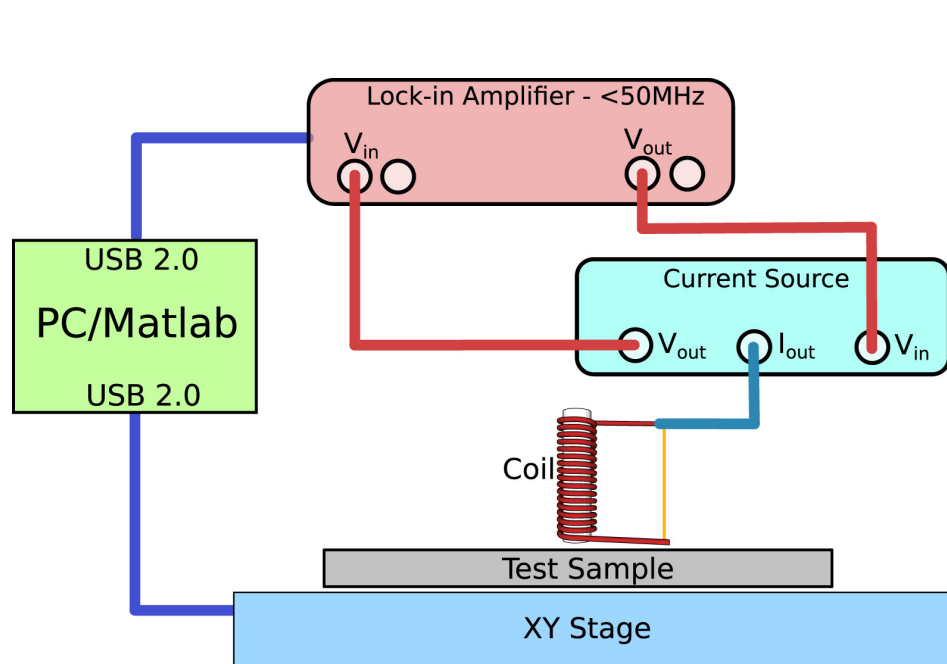
Cheng, Jun, et al. NDT & E International 119 (2021): 102403.

$$n_c \times (E_2 - E_1) = 0 \Rightarrow E_{2\tau} = E_{1\tau},$$

where  $n_c$  is the normal vector on the interface boundary, and the subscript  $\tau$  represents the tangential component.

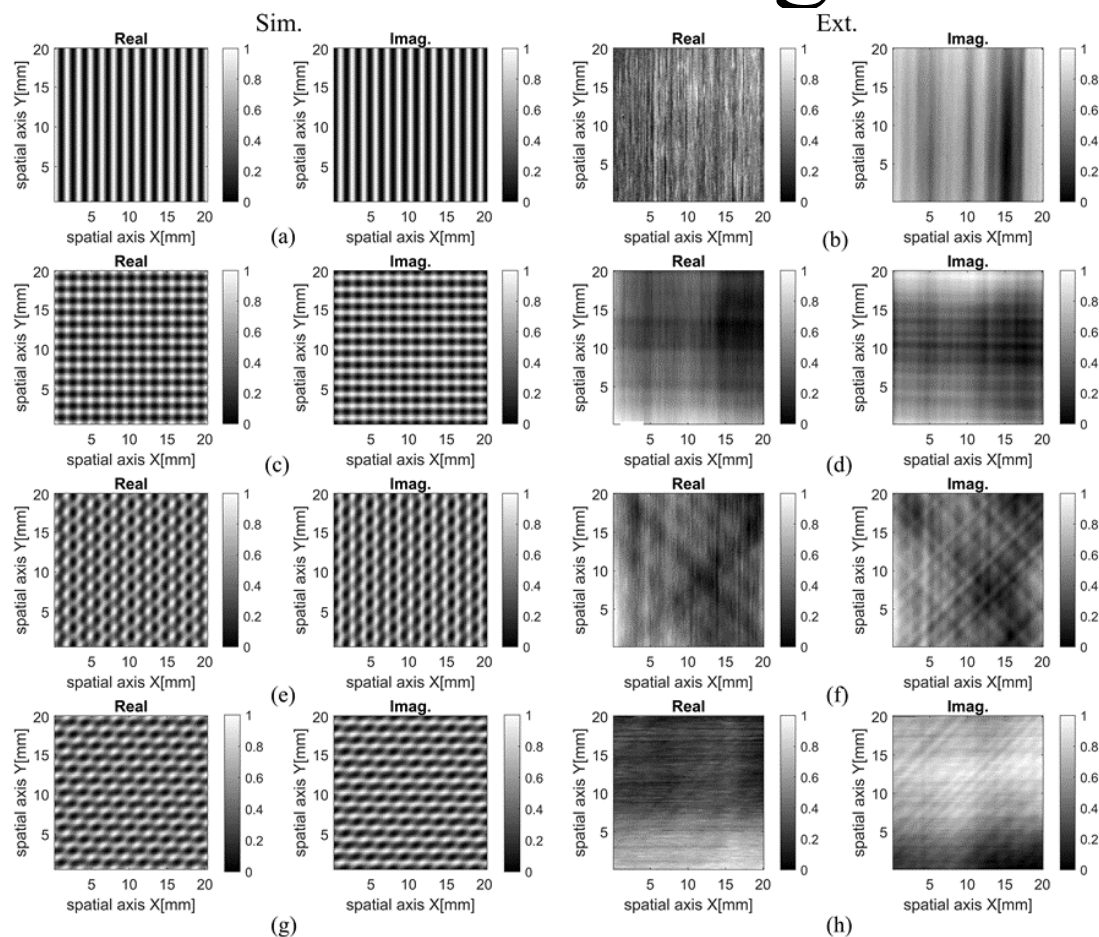
In-plane  $E$  can circulate in the two principal fibre directions to form a closed loop, greatly reducing the resistive loss and significantly increasing the current density

# Samples and experimental ECT system



#	Orientations	Structure	No. Layers	Thickness (mm)	Material
001	[0]	Unidirectional	32	4	IM7 8552 Prepreg
002	[0/90]	Bi-directional	32	4	IM7 8552 Prepreg
003	[90/45/90/-45]	Reflected	32	4	IM7 8552 Prepreg
004	[0/45/90/-45]	Repeated	32	4	IM7 8552 Prepreg

# Results-Modelling vs. Expt.



**A. CORR2(REAL)**

	001_E	002_E	003_E	004_E
001_S	<b>0.37</b>	0.06	0.1	-0.08
002_S	0.26	<b>0.72</b>	0.08	-0.15
003_S	0.16	-0.17	<b>0.48</b>	0.13
004_S	0.17	0.04	0.12	<b>0.38</b>

**B. CORR2(IMAG.)**

	001_E	002_E	003_E	004_E
001_S	<b>0.42</b>	-0.14	-0.11	0.08
002_S	-0.33	<b>0.88</b>	0.39	0.17
003_S	-0.2	0.12	<b>0.51</b>	0.09
004_S	-0.16	-0.06	0.12	<b>0.59</b>

**C. CORR2 (Real vs. IMAG.)**

	001_S.Im	002_S.Im	003_S.Im	004_S.Im
001_S.Re	<b>-0.98</b>	-0.4	-0.85	-0.13
002_S.Re	-0.56	<b>-0.96</b>	-0.49	-0.77
003_S.Re	-0.71	-0.29	<b>-0.95</b>	-0.38
004_S.Re	-0.22	-0.79	-0.45	<b>-0.96</b>

$\Delta L = L'_0 - L_0 = -\Delta R \frac{L_e}{R_e}$

# Results-orientation analysis in modelling and experiments

- 1 [90]

---

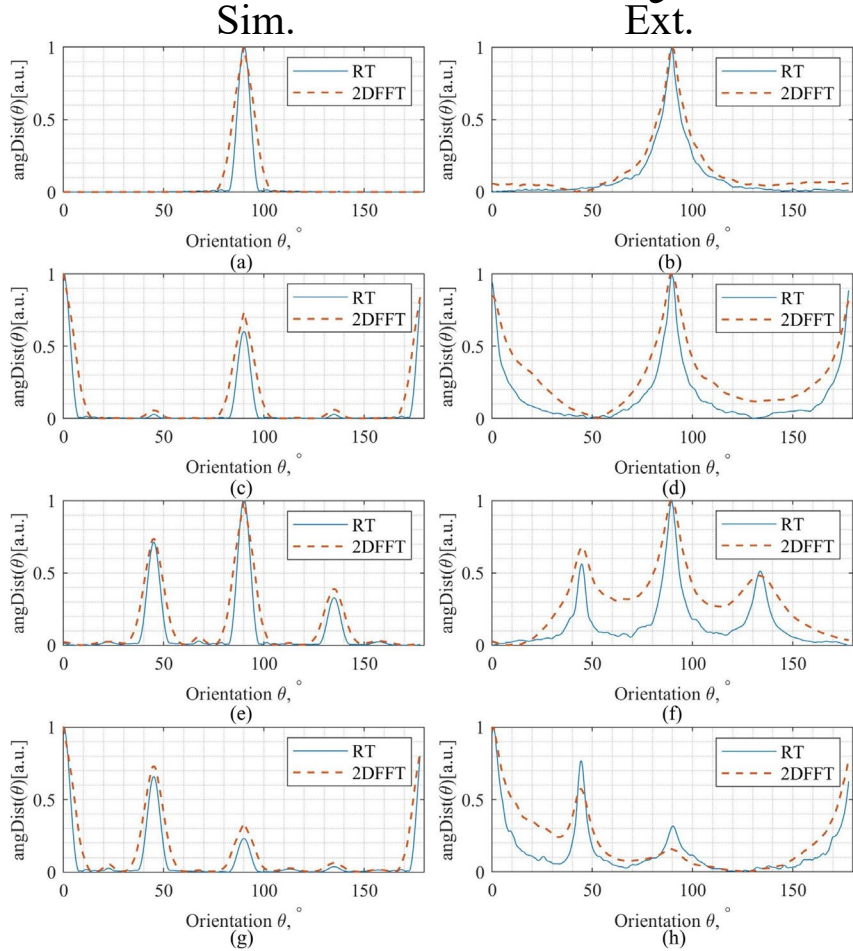
- 2 [0/90]

---

- 3 [90/45/90/-45]

---

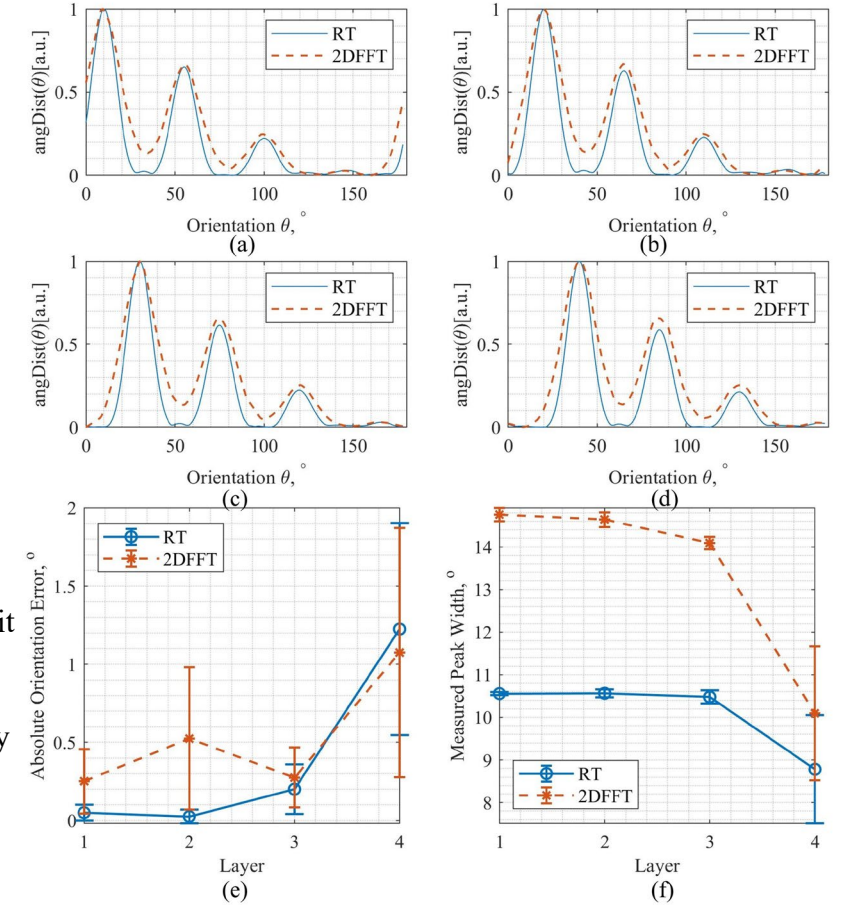
- 4 [0/45/90/-45]



offsets of  
 $10^\circ, 20^\circ, 30^\circ$  and  $40^\circ$

Minimize the bias  
to  $0^\circ/90^\circ$

The RT techniques exhibit  
greater angular  
measurement accuracy,  
precision and consistency  
over 2D FFT

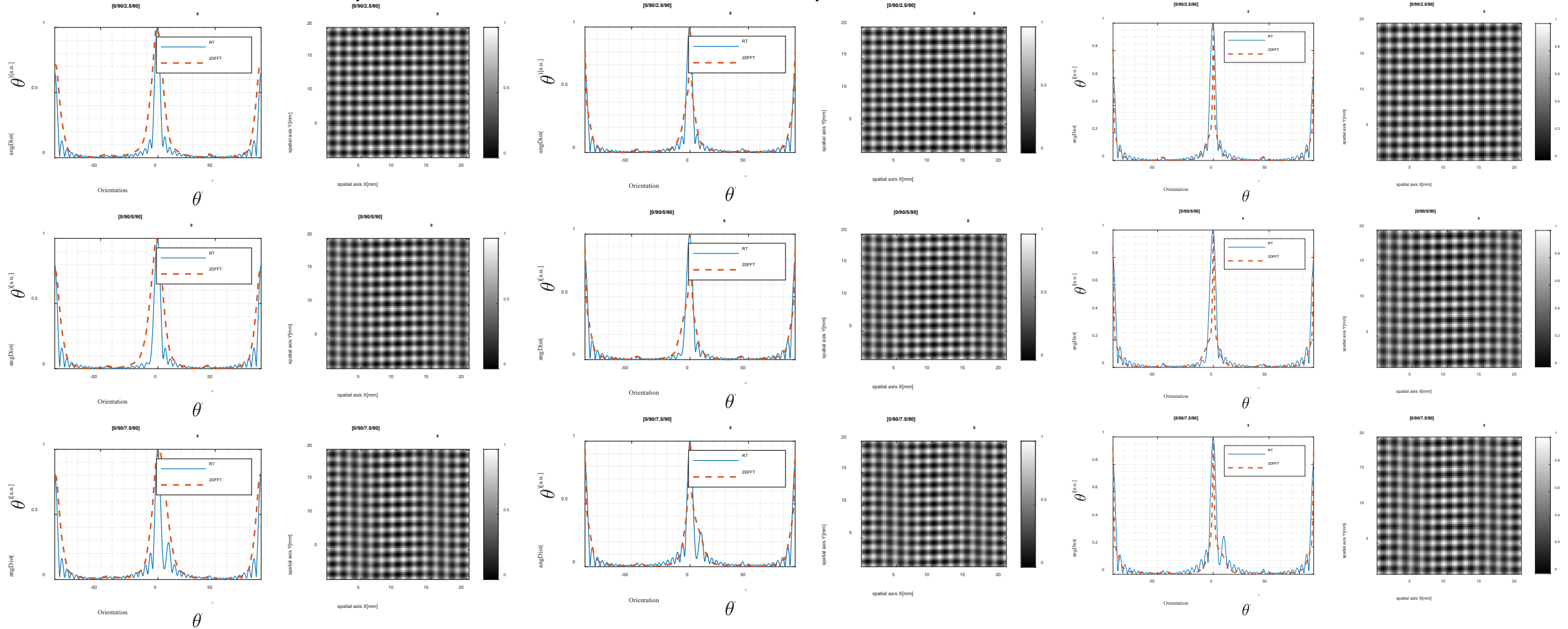


# Virtual misalignment detection

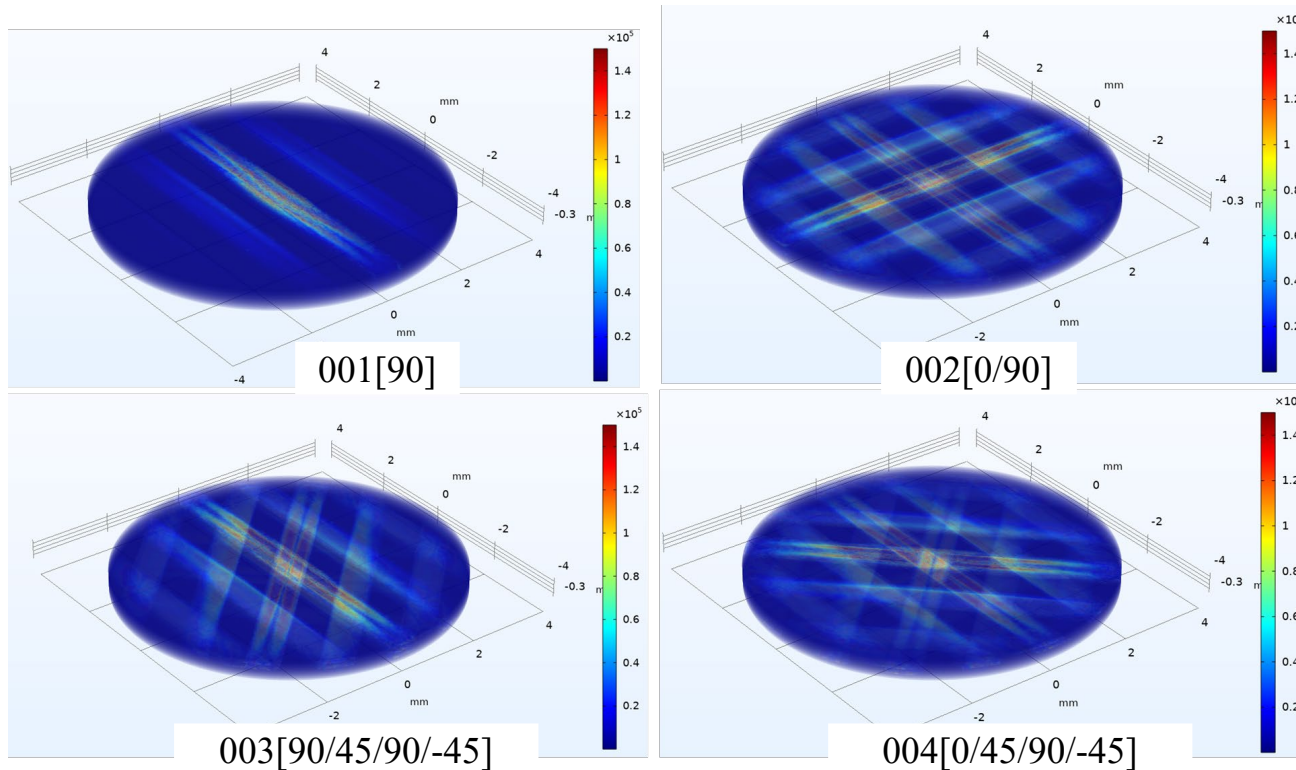
No 2D interp

2x interp.

4x interp.



# Results-resistivity loss(skin-depth) in multi-layer structure



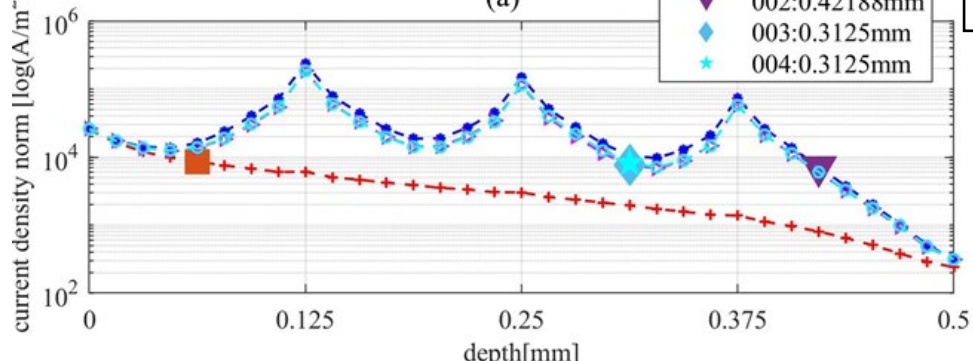
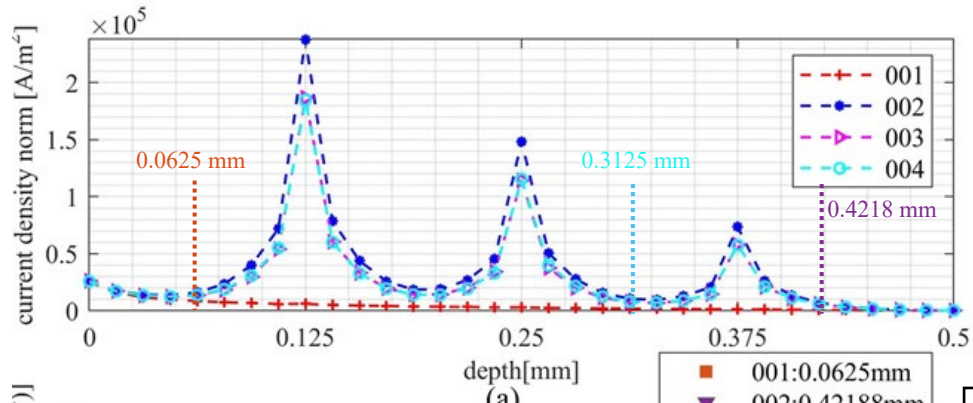
Current density in simulated structures

The traditional skin depth

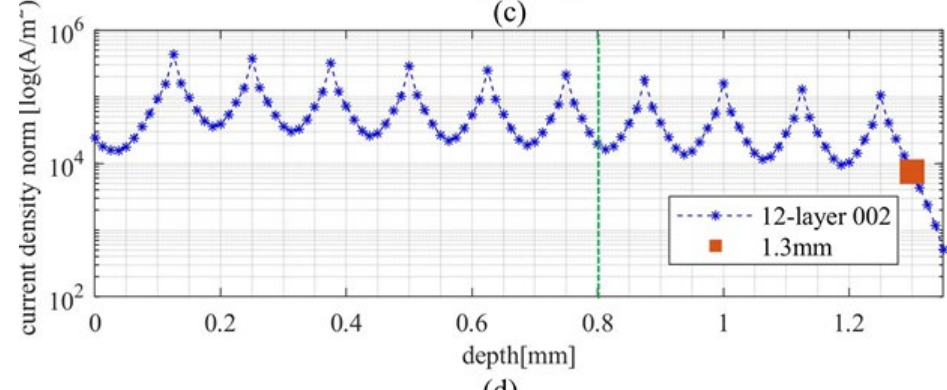
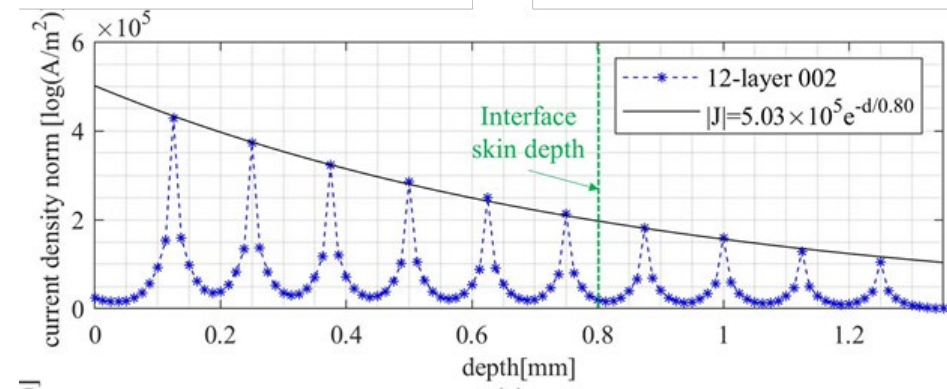
$$|J| = J_0 e^{-d/\delta_e}$$

- One of the critical parameters for eddy current testing is the skin depth.
- To do this, a finer mesh is used in the depth direction and the current density norm is averaged on 4mm radius planes.
- The mesh is scaled to 9 tetrahedral elements in each layer to provide 33 planes over a 0.5 mm depth range with a step of 0.0156 mm.

# Results-resistivity loss(skin-depth) in multi-layer structure



Traditional skin depth



Interface skin-depth calculated using interface current density

$$\delta_e = \frac{\Delta d_n}{\ln \left\{ \frac{|J_{n1}|}{|J_{n2}|} \right\}}$$

↓

$$\delta_e = 0.80 \text{ mm}$$

$$\delta_e = \sqrt{2 / \mu \sigma_e \omega}$$

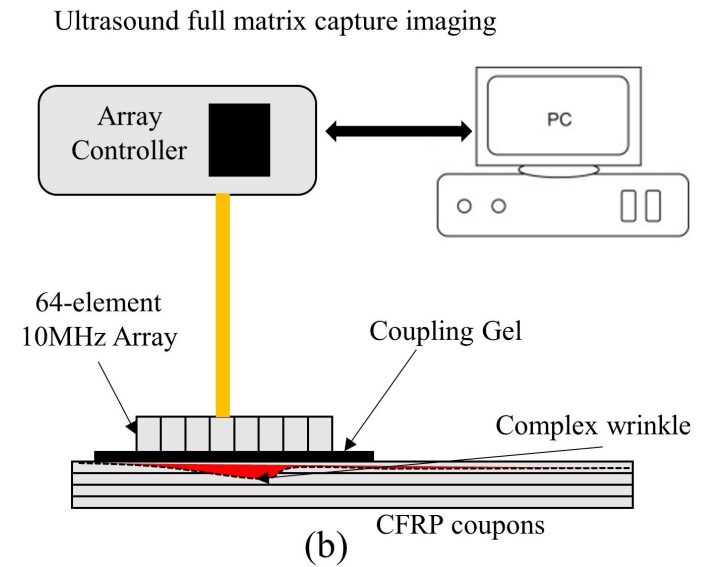
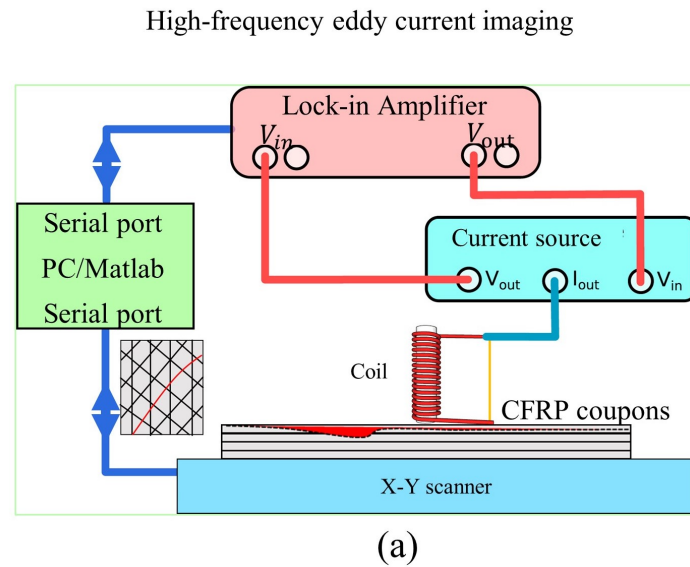
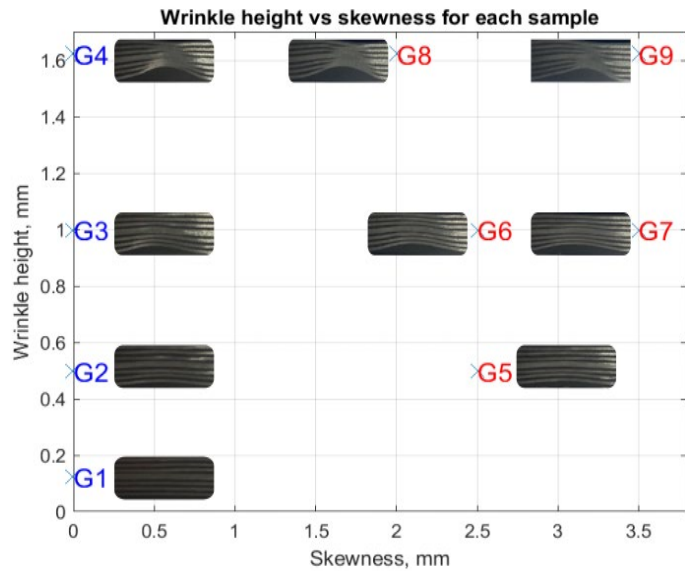
$$\sigma_e = 19,890 \text{ S/m}$$

$$\approx 1/2 \text{ of } \sigma_L$$

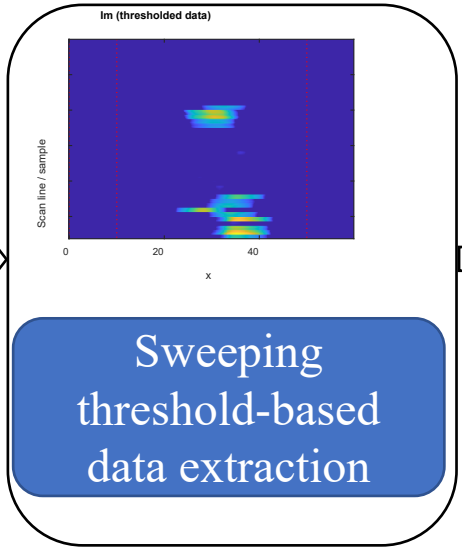
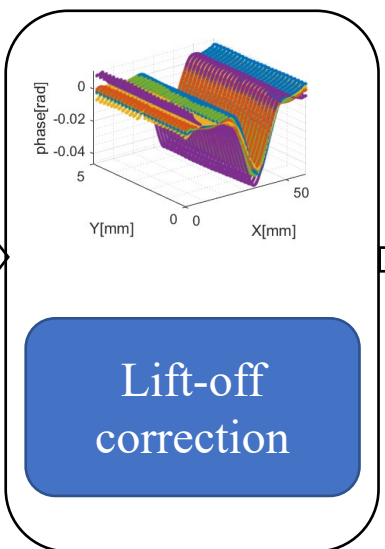
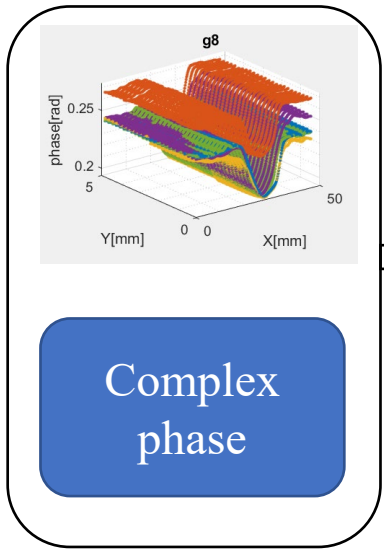
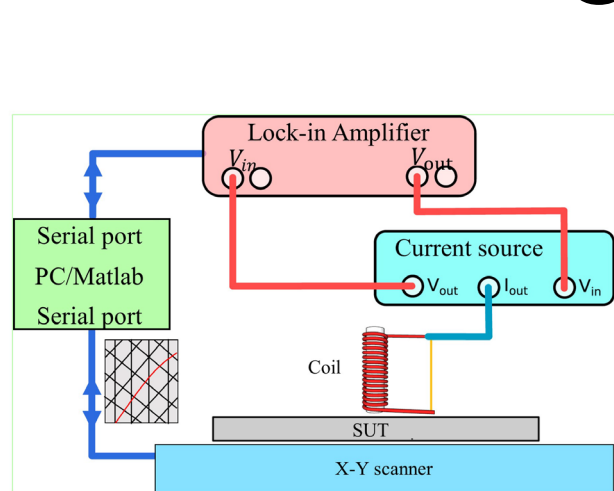
With a rapidly oscillating current density, the traditional skin depth is random and doesn't have the same physical meaning as in a homogeneous sample

# Application to asymmetric wrinkles

- To demonstrate the workflow of using both high frequency eddy current and ultrasound on the same defects and how to quantitatively compare their detectability and performance.
- The wrinkle geometries can be challenging to be evaluated due to it is related with multiple parameters such as asymmetry, wavelength, and amplitude affecting the mechanical performance of the structure



# Methodology-high frequency eddy current



Skew: Probability density function moment

Amplitude: Real or Imaginary peak values

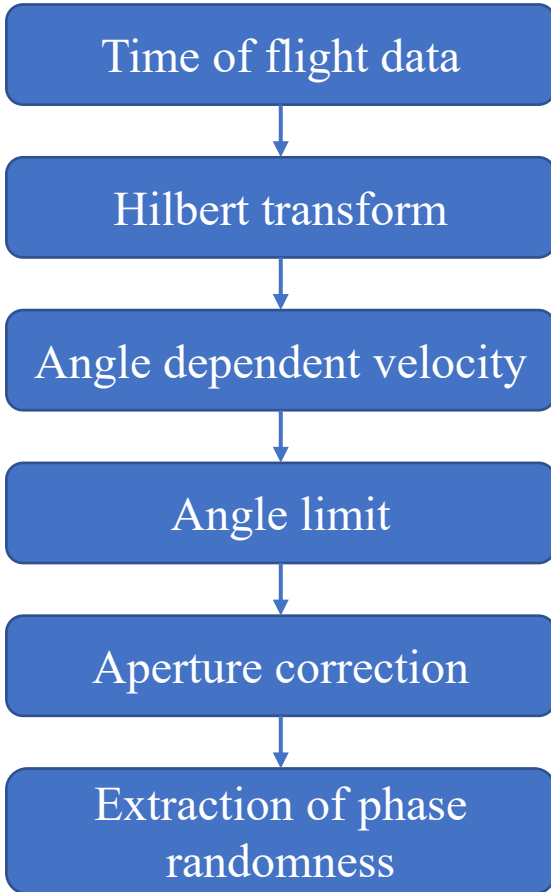
Wrinkle skew calculation method for characterisation

Should be independent of number of points considered – therefore should be performed on thresholded data (so that number of zeros outside thresholded region does not affect result)

Using following (applied separately to real and imag parts of data,  $z_i$ )

$$skew = \sqrt[3]{\frac{\sum_i (x_i - \mu_x)^3 z_i}{\sum_i z_i}}, \mu_x = \frac{\sum_i x_i z_i}{\sum_i z_i}$$

# Methodology-Ultrasound



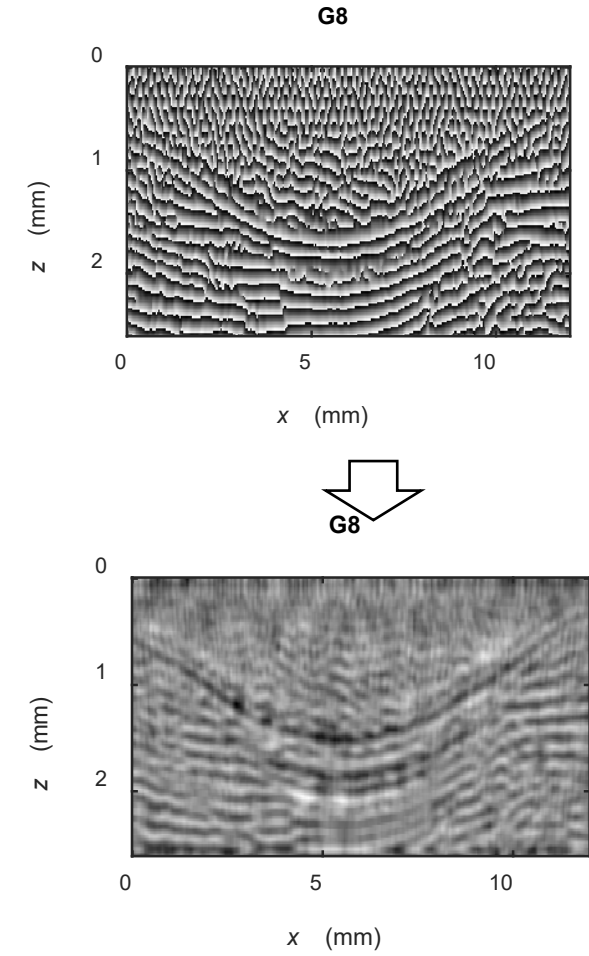
$$H_{ij}(\omega) = \int_{-\infty}^{\infty} h_{ij}(t) \exp(-i\omega t) dt$$

$$c(\theta) = \sum_{k=0}^3 a_k \theta^k$$

$$t_{ij}(\mathbf{r}) = \frac{|\mathbf{x}_i - \mathbf{r}|}{c(\theta_i)} + \frac{|\mathbf{x}_j - \mathbf{r}|}{c(\theta_j)}$$

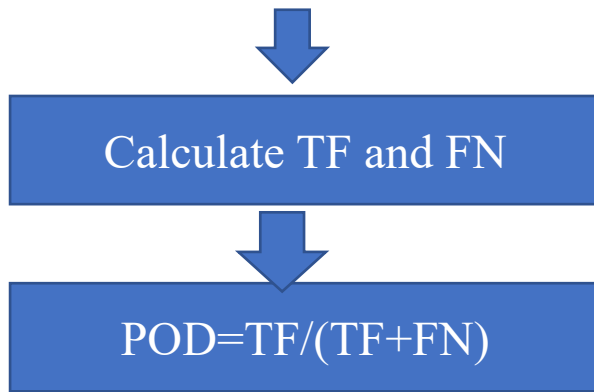
$$A(z) = 2z \tan \theta_{cap}$$

$$E(x, z) = -\log_2 \left( \frac{\phi(x, z)}{\sum_{x_c - k/2 < x < x_c + k/2} \phi(x, z)} \right)$$



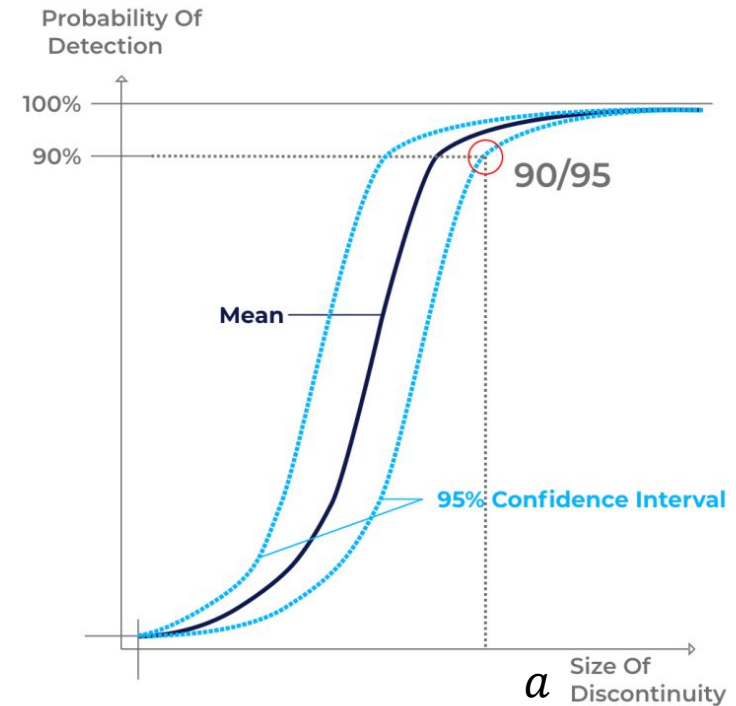
# Methodology-Probability of Detection

$$Y = \begin{cases} 1(\textit{hit}), & (1 - r) * a_0 < a < (1 + r) * a_0 \\ 0(\textit{miss}), & \textit{not in the region} \end{cases}$$



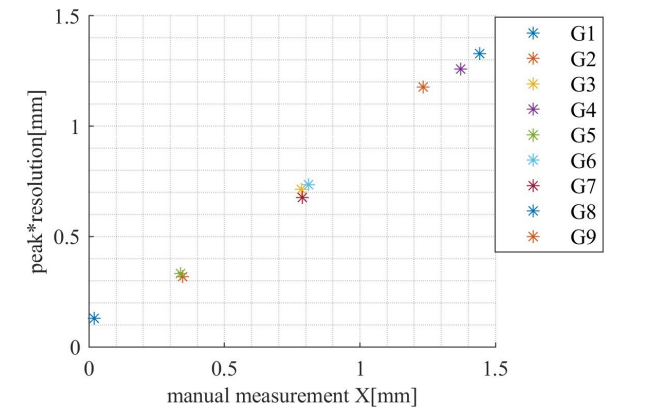
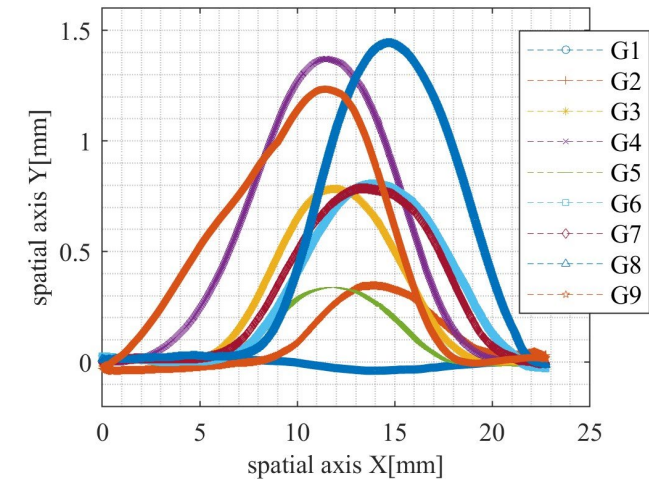
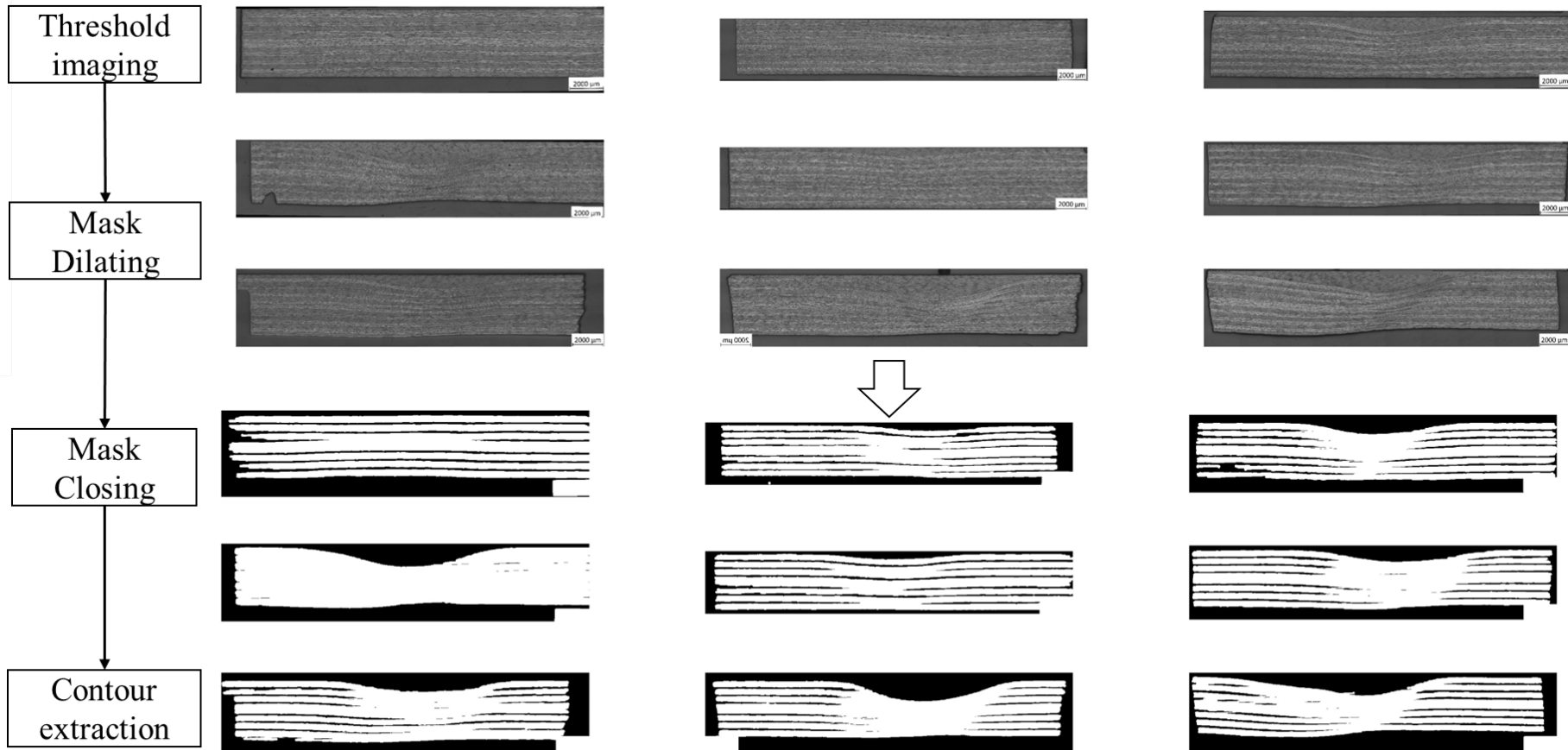
Then fit using logit function

$$POD(a) = \frac{\exp\left(\frac{\ln a - u}{\sigma}\right)}{1 + \exp\left(\frac{\ln a - u}{\sigma}\right)}$$

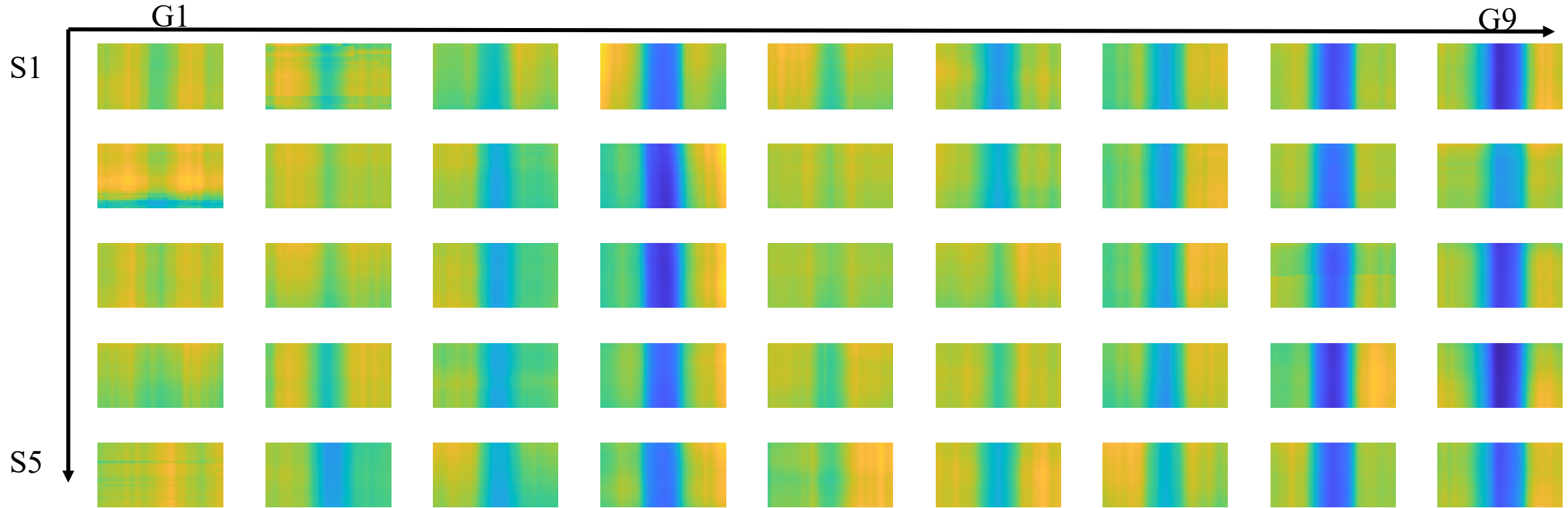


Could be skewness or amplitude

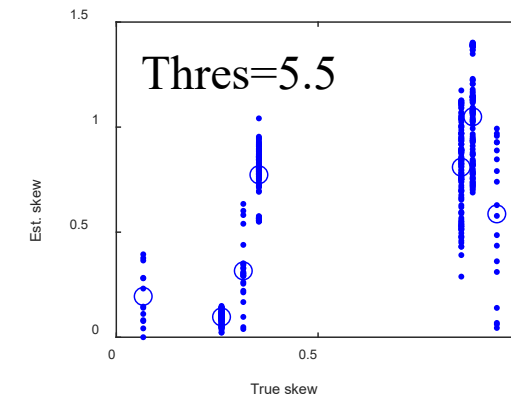
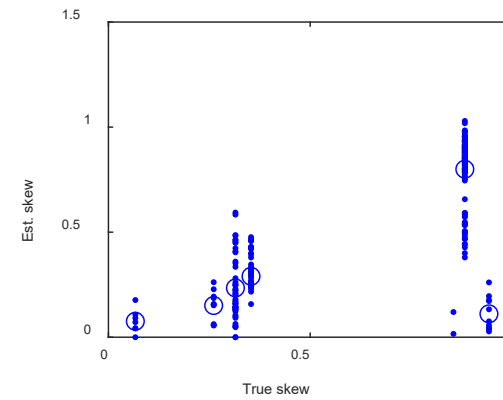
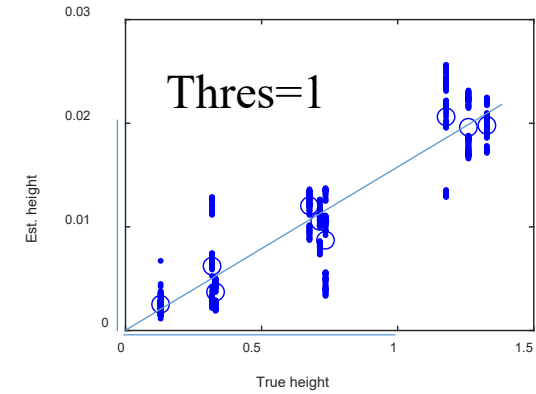
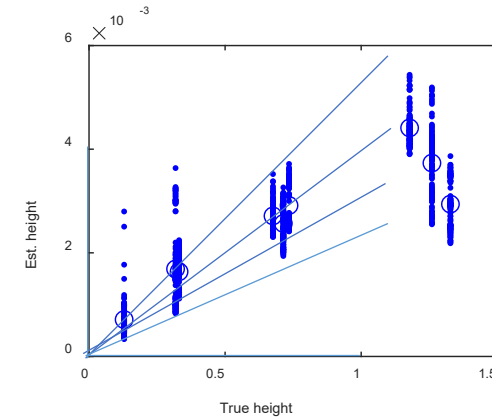
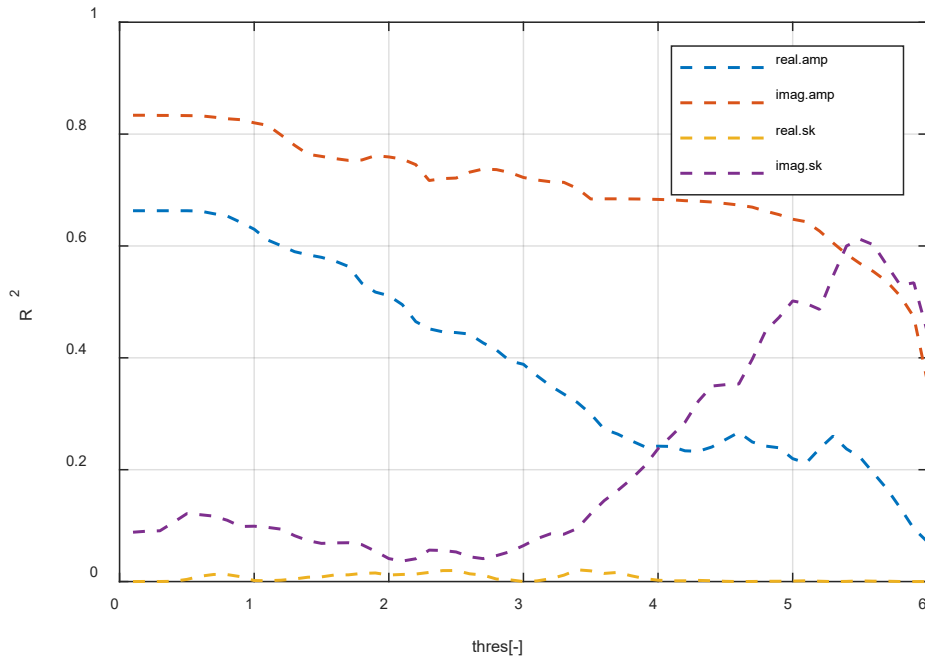
# Results analysis-obtaining ground truth



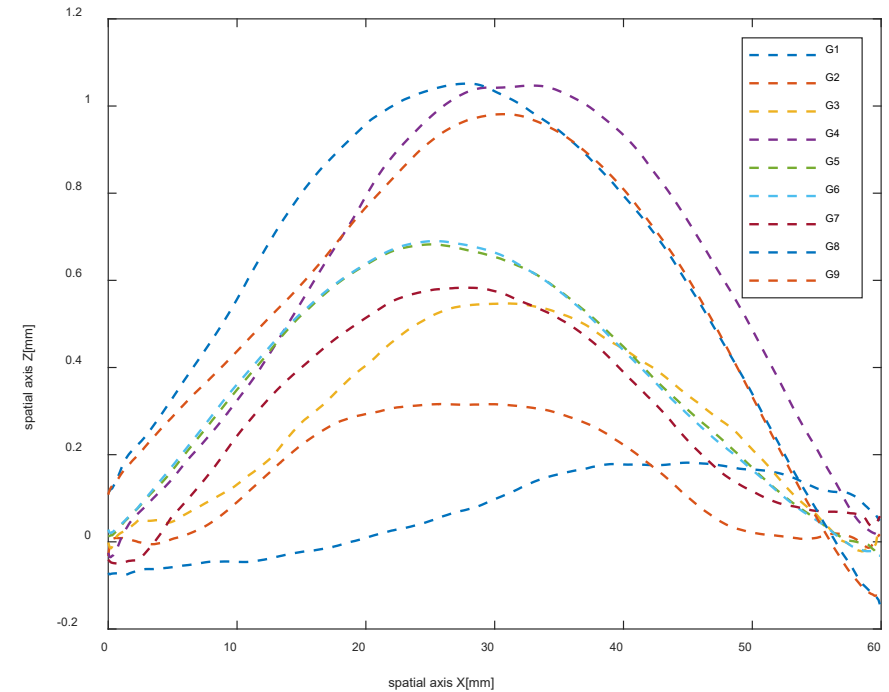
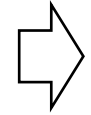
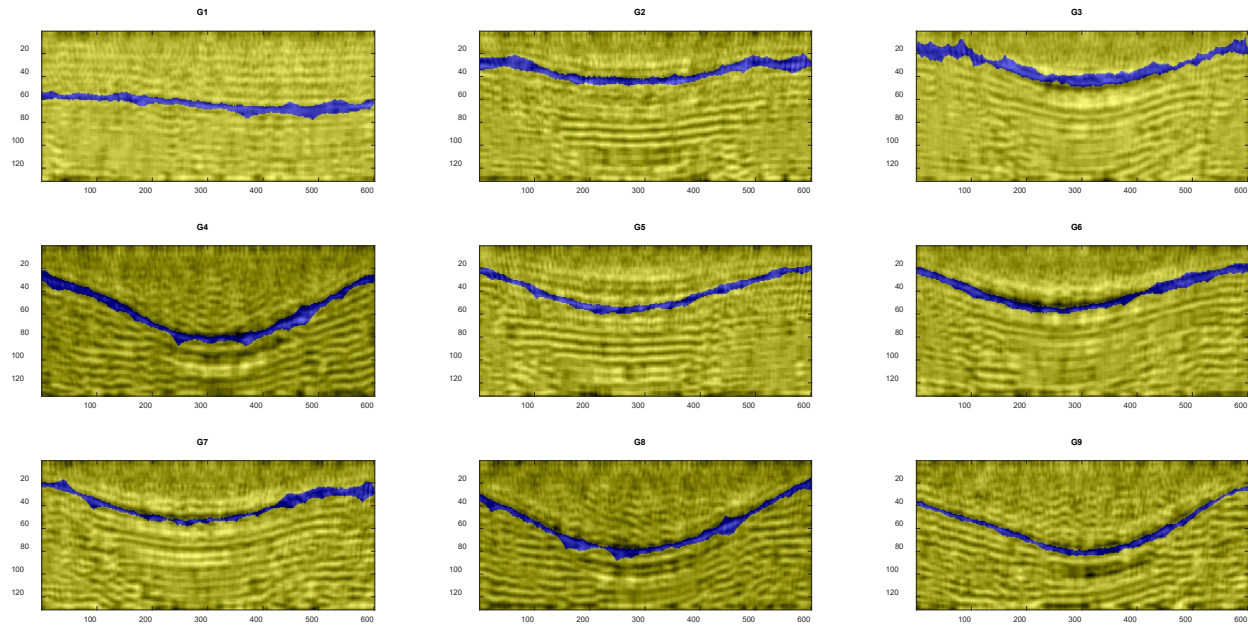
# Results analysis-eddy current raw data



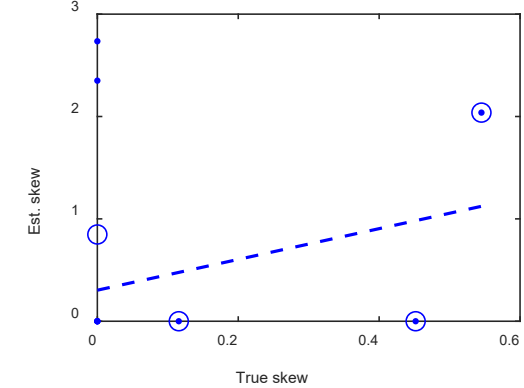
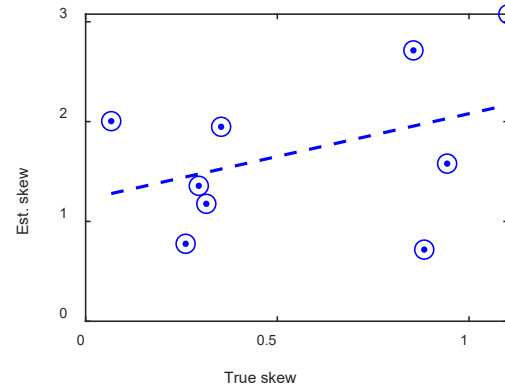
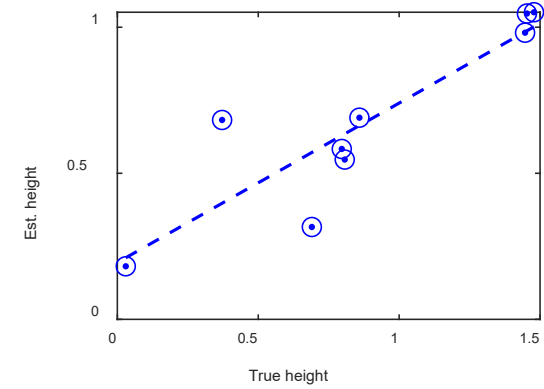
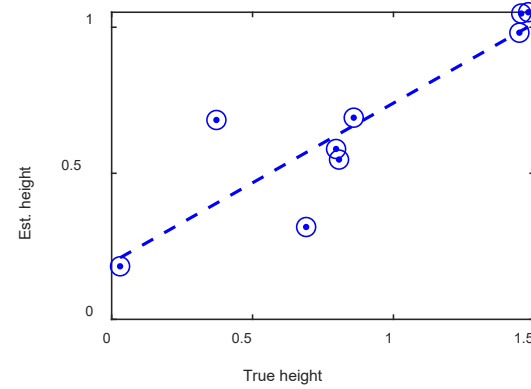
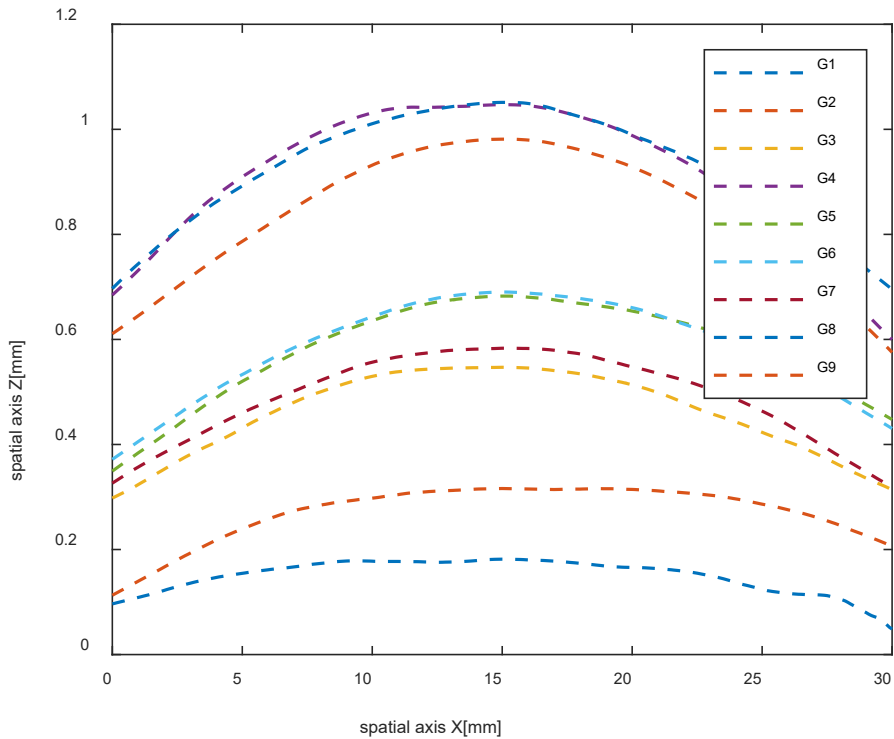
# Results analysis-eddy current data analysis



# Results analysis-UT raw data

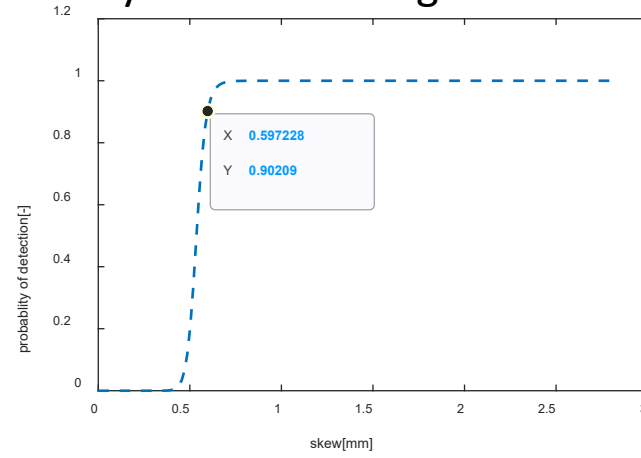
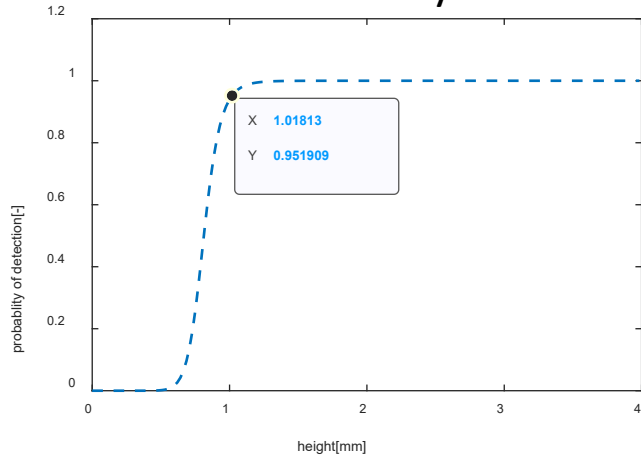


# Results analysis-UT data analysis

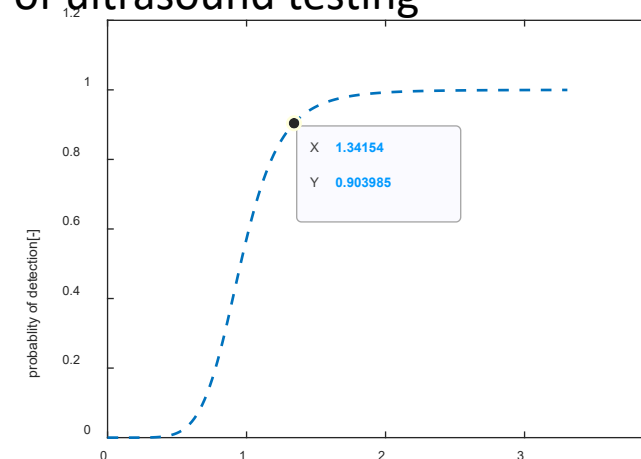
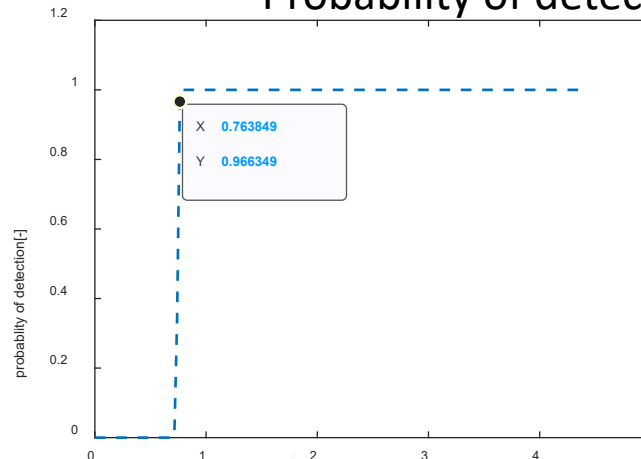


# Results analysis-UT compare with EC

Probability of detection of eddy current testing

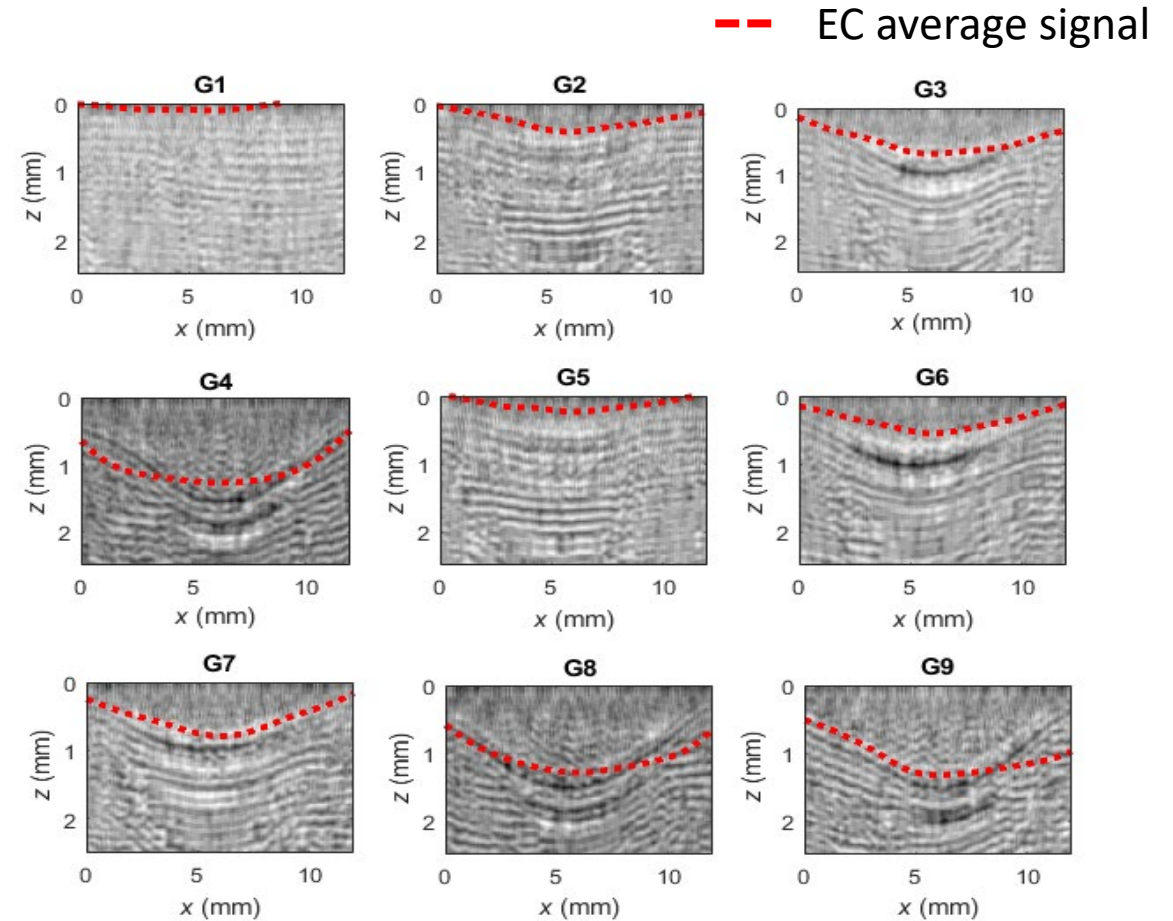


Probability of detection of ultrasound testing



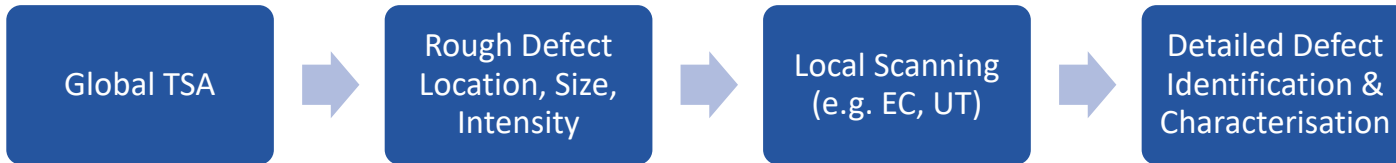
# Results analysis- “Fusing” UT with EC

- UT and EC have the potential to be merged to achieve improved characterisation of wrinkle defects.
- The average EC signal from all samples shows decent agreement in most cases with the UT generated images.
- EC allows better detection of near-surface defects (G1) and better detection of asymmetry.
- **Still to be explored:**
  - Robust co-location, co-orientation, and merging of signals into singular wrinkle description.
  - Viability of data fusion for more complex defect states (i.e. requiring separation of defect type signatures).

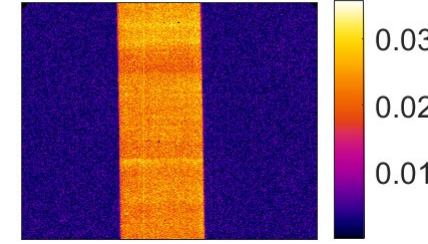


# The opportunity for TSA

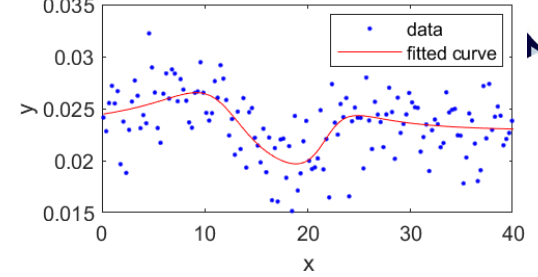
- Thermo-elastic Stress Analysis (TSA) offers a flexible approach to identify regions of interest within a structure.
- For the “simple” case of the asymmetric wrinkle coupons, TSA with some processing appears able to detect the presence of wrinkles from both sides even for the smallest deviation (1 ply thickness).
- Basic analysis also show good match for wavelength ( $\approx 10\text{mm}$ ) and further analysis is ongoing.
- Hence, opportunity for rough defect localization, and indication of size and “severity” on global scale appears very promising.



Processed Temperature Field

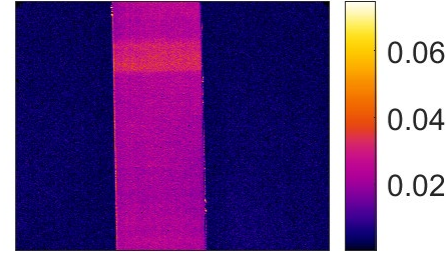


Vertical Midline

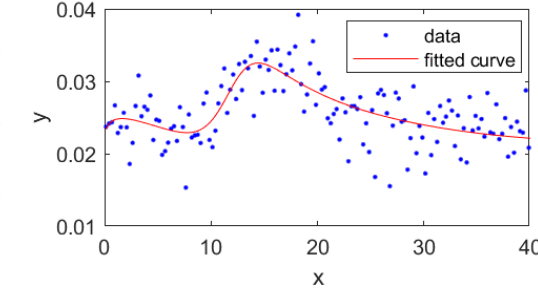


G1 S2 – Bag Side

Processed Temperature Field

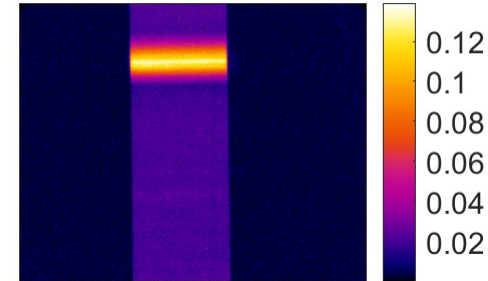


Vertical Midline

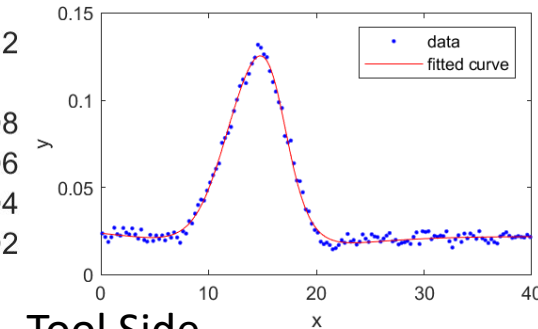


G1 S2 – Tool Side

Processed Temperature Field



Vertical Midline



G8 S2 – Tool Side

# Conclusion

- Eddy current modelling

- The proposed modelling advance offers improved computation speeds and the potential to simulate the eddy-current inspection of anisotropic structure as well as facilitating the virtual design and optimisation of high-frequency ECT inspections in the future.
- The angular distribution analysis using Radon transform (RT) and 2D-FFT has also demonstrated its capability to automatically validate models and characterise ply orientations from both simulated and experimental complex ECT scan data.
- A new parameter referred to as the interface skin-depth is defined and calculated based on the decay in current density at the interfaces and used to determine an approximate effective conductivity of the layered structures.

- Wrinkle NDT&E

- The wrinkle profiles are successfully extracted from three systems including high frequency data, UT data and micrographs.
- The probability of detection study reveals the merits of UT for detecting the wrinkle amplitude while EC is more sensitive to the asymmetry, due to that wrinkle asymmetry contributes more to electrical properties change than that of stiffness.